

1 **Chromium VI adsorption on cerium oxide nanoparticles and morphology changes**
2 **during the process**

3

4 Sonia Recillas^a, Joan Colón^a, Eudald Casals^b, Edgar González^b, Victor Puntès^{bc}, Antoni
5 Sánchez^{a*}, Xavier Font^a

6

7 ^a Department of Chemical Engineering, Engineering School, Autonomous University
8 of Barcelona, 08193 Bellaterra, Spain.

9 ^b Catalan Institute of Nanotechnology, Autonomous University of Barcelona Campus,
10 08193 Bellaterra, Spain.

11 ^c Catalan Institute of Research and Advanced Studies, Passeig Lluís Companys, 23,
12 08010 Barcelona, Spain.

13

14

15 * Corresponding author: Antoni Sánchez

16 Phone: 34-9358141019

17 Fax: 34-935812013

18 E-mail address: antoni.sanchez@uab.cat

19

20

Pre-print of: Recillas, S. et al. "Chromium VI adsorption on cerium oxide nanoparticles and morphology changes during the process" in Journal of hazardous materials (Ed. Elsevier), vol. 184, issues 1-3 (Dec. 2010), p. 425-431.

The final version is available at DOI 10.1016/j.hazmat.2010.08.052

21 **Abstract**

22

23 In this study, suspended cerium oxide nanoparticles stabilized with
24 hexamethylenetetramine were used for the removal of dissolved chromium VI in pure
25 water. Several concentrations of adsorbent and adsorbate were tested, trying to cover a
26 large range of possible real conditions. Results showed that the Freundlich isotherm
27 represented well the adsorption equilibrium reached between nanoparticles and
28 chromium, whereas adsorption kinetics could be modeled by a pseudo-second order
29 expression. The separation of chromium-cerium nanoparticles from the medium and the
30 desorption of chromium using sodium hydroxide without cerium losses was obtained.
31 Nanoparticles agglomeration and morphological changes during the adsorption-
32 desorption process were observed by TEM. Another remarkable result obtained in this
33 study is the low toxicity in the water treated by nanoparticles measured by the
34 Microtox® commercial method. These results can be used to propose this treatment
35 sequence for a clean and simple removal of drinking water or wastewater re-use when a
36 high toxicity heavy metal such as chromium VI is the responsible for water pollution.

37

38

39 **Keywords:** CeO₂ nanoparticles, adsorption, desorption, kinetics, chromium VI, toxicity.

40

41

42

43 **1. Introduction**

44 Water treatment is one of the main health concerns around the world. The world's
45 supply of fresh water is running out. Already one person in five has no access to safe
46 drinking-water. Improving access to safe drinking-water can result in tangible
47 improvements to health. Therefore the development of new technologies to improve
48 process of products in the area of water treatment is fundamental. One of the promising
49 technologies is based on nanotechnology devices and products. Nanotechnology is the
50 engineering of functional systems at the molecular scale, synthesized "bottom-up",
51 which offer new products and process alternatives for water purification, being the
52 advantage of these materials the large surface to volume ratio [1].

53 Some examples of nano-devices proved in water treatment are based on
54 nanoparticles, nanomembranes, bioactive nanoparticles, carbon nanotubes and
55 nanofibers [2-5]. In the future, the impact of these nanomaterials on human health and
56 environment would be critical issues involving the materials and process selection for
57 water purification on large scale [6].

58 Chromium (VI) is one of the contaminants that has been used as target pollutant
59 due to its high toxicity and also for the well-documented human health problems
60 associated to chromium [7]. The amount of chromium (Cr) allowed in purified water is
61 very low (50 $\mu\text{g/l}$ according to the Council of the European Union [8]). A variety of
62 products and processes have been used for chromium removal in water [9]; nevertheless
63 the adsorption process is one of the more effective and versatile techniques for Cr
64 removal from water and when combined with an appropriate desorption step the
65 problem of sludge disposal could be solved [10]. The absorbents used for Cr(VI)
66 removal are alumina, silica [11, 12], activated carbon [13, 14] or natural adsorbents
67 [15]. In the field of nanotechnology amino-functionalized magnetic nano-adsorbents

68 [16], iron nanoparticles, cerium micro/nanocomposite structures [17] or carbon
69 nanotubes supporting cerium nanoparticles [18] have been used. Cerium nanocrystal
70 microspheres [19] have been also synthesized and tested with the same objective.

71 Cerium nanoparticles have been used in a variety of industrial applications such
72 as catalysis, solar energy devices, optical display technology and corrosion prevention
73 [20, 21]. All of these applications are related with chemical reaction at the surface,
74 while cerium nanoparticles reactivity is correlated to surface defects.

75 Another important issue is to determine the toxicity of the synthesized materials
76 and the prevention of future environmental damages. The Microtox® assay based on the
77 use of bioluminescent marine bacterium, *Photobacterium phosphoreum*/ *Vibrio fischeri*,
78 adopted for the assessment of toxicity of polluted water [22] is commonly used to test
79 detoxification efficiency.

80 In the present paper CeO₂ nanoparticles (6.5 nm mean size) were synthesized
81 and fully characterized to be used as adsorbent for the removal of chromium (VI) from
82 pure water solutions. The adsorption isotherms at 0.6, 37.5, 80 mg/l initial chromium
83 (VI) concentrations were obtained and different eluents were tested for the chromium
84 (VI) desorption. Because the application would be for drinking or natural water
85 treatment technologies, the experiments were performed at pH = 7. The changes in
86 morphology during the adsorption-desorption process were studied by Transmission
87 electron microscopy. The toxicity of the decontaminated effluents was also studied
88 using the Microtox assay to evaluate the overall possibilities of this treatment.

89

90 **2. Materials and Methods**

91

92 *2.1. CeO₂ Nanoparticles preparation*

93 CeO₂ nanoparticles were synthesized in aqueous phase, using milli-Q grade water. All
94 reagents were purchased from Sigma-Aldrich and used as received. All the synthesis
95 procedures are based in preexisted ones available in the scientific literature with
96 modifications to be adapted to large-scale yields. Briefly, CeO₂ nanoparticles synthesis
97 was based on Zhang et al. [23]. The Ce³⁺ ions from Ce(NO₃)₃ salt are oxidized at basic
98 pH conditions to Ce⁴⁺ using Hexamethylenetetramine (HMT). Specifically, stock
99 solutions of 1M of both reactants were prepared and stored at room temperature.
100 Afterwards, both were mixed and stirred during 24 hours at final concentrations of 37.5
101 mM for Ce(NO₃)₃·6H₂O and 0.5 M for HMT, under mild stirring and room temperature
102 conditions. In this process, CeO₂ nanocrystals form and the same reagent (HMT)
103 stabilize them in aqueous medium, forming the double electrical layer to prevent
104 nanoparticles agglomeration.

106 *2.2. Characterization and stability of nanoparticles*

107 For the fully characterization of nanoparticles, the obtained nanoparticles suspension
108 was analyzed with dynamic light scattering (DLS) to determine the nanoparticles size
109 distribution (and therefore if agglomeration had occurred) in a Nanoparticle Analysis
110 System (Malvern, UK). DLS is a well-known tool to determine the hydrodynamic
111 diameter of colloidal particles.

112 Zeta Potential (ZP) measurements were also performed to study some surface
113 properties and changes after the experiments. ZP is a useful technique to study
114 nanoparticles stability and their surface charge in colloids when they are
115 electrostatically stabilized.

116 X-Ray Diffraction spectra (using a PANalytical X'Pert diffractometer with a Cu
117 K α radiation source) have also been taken to determine the crystalline phase of the

118 samples.

119 The dissolved cerium concentration from the desorption experiments was
120 obtained by Inductively Coupled Plasma Mass Spectrometry (ICP-MS) using an Agilent
121 Equipment (Model 7500ce).

122 Transmission electron microscope (TEM, using a JEOL 1010 operating at an
123 accelerating voltage of 80 kV) images of the samples were also taken after nanoparticles
124 synthesis, to characterize the nanoparticles before and after the chromium adsorption
125 process.

126 Table 1 shows some of the main characteristics of the used nanoparticles as they
127 were synthesized.

128

129 *2.3. Cr(VI) Adsorption studies*

130 The adsorption kinetics, the maximum adsorption capacity (q_e) of CeO₂ nanoparticles
131 synthesized at different initial concentration of chromium (VI) at pH=7, were performed
132 using the following procedure: chromium (VI) solutions were prepared dissolving
133 K₂Cr₂O₇ in deionized water and performing the corresponding dilutions to obtain 0.6,
134 37.5 and 80 mg/l solutions. The pH of each solution was adjusted at 7 using sodium
135 hydroxide 1M. Each of these solutions was added to equal volumes of CeO₂
136 nanoparticles suspension adjusted to pH=7 and then the solutions were continuously
137 stirred at 150 rpm at room temperature. Final concentration of CeO₂ nanoparticles was
138 320 mg/l. Samples were taken at different times, separated by centrifugation and Cr(VI)
139 was analyzed in the liquid phase.

140 The method used for the determination of Chromium total was the standard
141 colorimetric method used for the examination of water and wastewater [24]. The
142 chromium VI concentration is determined colorimetrically by reaction with

143 diphenylcarbicide in acid solution. The reaction is very sensitive; being the molar
144 absorptivity based on chromium about $40,000 \text{ L g}^{-1}\text{cm}^{-1}$ at 540 nm. To determine total
145 chromium, the sample was digested with a sulphuric-nitric acid mixture to oxidize with
146 potassium permanganate before reacting with the diphenylcarbicide. The determination
147 of trivalent chromium on the liquid phase was performed by oxidation with potassium
148 permanganate as follow: 1 ml of sample was added into a 125 ml conical flask. Acid
149 sulphuric-nitric (1:1, v:v) solution was added dropwise until the solution is acid, plus 1
150 ml in excess, the volume was adjusted to 40 ml and heat to boiling. Two drops of
151 KMnO_4 solution were added and the resulting solution was boiled for two minutes
152 more. 1 ml NaN_3 solution was added. The sample continued boiling for 1 min after
153 colour has faded completely. The sample was cooled and then the process for the
154 determination of Cr VI is performed. The Chromium IV determination was obtained as
155 follow: 1 ml of sample was added into a 100 ml flask, 0.25 ml H_3PO_4 was added and the
156 pH was adjusted to 1.0 ± 0.3 with a 0.2N H_2SO_4 solution. The solution was transferred
157 to a 100 ml flask, diluted to 100 ml, and mixed. 2.0 mL diphenylcarbicide solution was
158 added, mixed and wait for 10 min for full colour development. An appropriate portion
159 of the sample was transfer to a 1-cm absorption cell and its absorbance was measured at
160 540 nm. The amount of Cr III in solution will be the difference between total chromium
161 (with oxidation step) and the Cr VI amount. No difference between the Cr VI and Cr
162 total was obtained in the liquid phase after centrifugation.

163 Experiments were carried out in triplicate and the average values are presented.

164 Standard deviation was very low (less than 5% in all cases) and it is not presented.

165

166 *2.4. Cr(VI) desorption studies*

167 Desorption study was performed using the following procedure. Samples of 0.7 ml of a
168 suspension of 640 mg/l CeO₂ nanoparticles previously adjusted at pH=7 were shaken
169 and then 0.7 ml of 80 mg/l of chromium (VI) solution were added. The suspensions
170 were stirred for three hours at 150 rpm at room temperature and then separated by
171 centrifugation. In three samples chromium (VI) was determined at the liquid phase. In
172 the remaining 15 samples, the solid phases were dried at room temperature for 24 hours.
173 1 ml of each eluent used (deionized H₂O, 0.1M HNO₃, 0.1M HCl, 0.1M H₂SO₄ and
174 0.1M NaOH) were added to the solid samples and then the suspensions were stirred for
175 three hours, separated by centrifugation and chromium (VI) was analyzed in the liquid
176 phase. The initial and final concentrations of chromium (VI) were obtained by the same
177 analytical method used for adsorptions studies. The amount of cerium in solution was
178 determined by ICP-MS. Experiments were carried out in triplicate and the average
179 values are presented.

180

181 2.5. Bioluminescent test

182 A Microtox Analyzer model 500 from Microbics Corporation was used. Whole Effluent
183 Toxicity (WET) test protocol was used to obtain the toxicity of the initial chromium
184 (VI) solution (30 mg/l), the initial nanoparticles suspension of CeO₂ (320 mg/l) and the
185 final suspension obtained after 3 hours of reactions at pH 7 and at room temperature.
186 The Microtox test is based on the percentage of decrease in the amount of light emitted
187 by the bioluminescent marine bacterium *Vibrio fischeri* (*Photobacterium phosphoreum*)
188 [22]. The light emitted reduction is directly related to the relative toxicity of the sample.
189 For the three suspensions the half maximal inhibitory concentration (IC₅₀) was
190 calculated. IC₅₀ is a measure of the effectiveness of a compound in inhibiting
191 biological or biochemical function and it was obtained from plotting the percentage of

192 luminescence reduction against concentration after 5 and 15 min incubation time. The
193 experimental procedure has been adopted from the official standards of several
194 countries [25, 26]. Toxicity tests for stabilizer samples and nanoparticles suspensions
195 samples were performed in triplicate. pH of stabilizers and nanoparticles suspension
196 samples was previously adjusted to 7. No visible precipitate was observed during the
197 adjustment. The procedure used is as follows: The pH of the samples was adjusted at
198 pH 7 with citric acid. 10 ml of samples was added to a vessel containing 0.2 g of NaCl
199 and mixed. 2,000 μL of the suspension were added to a tube test. 1000 μL of diluent
200 were added to each test tube. Afterwards, 1,000 μL of osmotically adjusted sample were
201 added to test tubes making 1:2 serial dilutions by transferring 1,000 μL , mixing after
202 each transfer. After 5 minutes, a vial of Microtox Acute Toxicity Reagent was
203 reconstituted in the following way: pouring the reconstitution solution (precooled at
204 4°C) into the opened vial, swirling the vial 3 or 4 times, then quickly pouring the
205 mixture back into the cuvette. Bacteria were thoroughly mixed using a pipette by
206 aspirating and dispensing 0.5 ml of solution at least 10 times. Reconstituted bacteria
207 should be used within 3 hours of reconstitution. Finally, 10 μL reagent are transferred
208 to each test tube and mixed in cuvettes by shaking. I_{15} light levels at 5 minutes and 15
209 minutes can be already read. The sample concentrations performed were 320, 160, 80,
210 40, 20 mg/ml.

211

212 **3. Results and discussion**

213

214 *3.1 Adsorption isotherms*

215 CeO_2 nanoparticles crystallize in a cubic fluorite structure and the predominant
216 crystallographic planes exposed at the surface in the synthetic procedure used are the

217 (111) (Figure 1), which are responsible of the catalytic behaviour [27]. The average
218 diameter obtained was 11.7 ± 1.6 nm of 6.5 nm (Table 1). The size distribution was
219 obtained after image analysis of different TEM images, counting at least 500 NPs
220 (Figure 1). These nanocrystals have more cerium atoms per unit of surface than oxygen
221 atoms, inversely to CeO₂ NPs (100)-terminated which are predominantly oxygen
222 terminated [28]. These are related with the storage and releasing of oxygen, and the
223 promotion of noble-metal activity and dispersion [29, 30]. Both phenomena are
224 controlled by the type, size, and distribution of oxygen vacancies as the most relevant
225 surface defects [31, 32].

226 The adsorption evolution through time, obtained at different concentration of
227 chromium (VI), is shown in Figure 2. A brown precipitate was observed in each case
228 before the first measure of Cr(VI) was made. In the three chromium concentration cases
229 the equilibrium concentration was reached almost immediately. After 30 min the
230 systems reached equilibrium and were stable with time. The removal efficiency after
231 four hours of adsorption were found to be 96.5 %, 67.8 % and 50.6 % and the maximum
232 adsorption capacity of Cr(VI) obtained after 24 hours were 1.88 mg Cr(VI)/g CeO₂
233 nanoparticles, 83.33 mg Cr(VI)/g CeO₂ nanoparticles and 121.95 mg Cr(VI)/g CeO₂
234 nanoparticles at the initial concentration of Cr(VI) of 0.6, 37.5, 80 mg/l respectively
235 (Figure 2). Three samples of CeO₂ NPs with adsorbed Chromium were centrifuged and
236 the total amount of Chromium and Chromium VI were obtained from the liquid and the
237 solid (previous dissolution in acid medium) phases. Cr VI was not detected in the solid
238 phase. The total Cr obtained was Chromium III. In the liquor phase only Chromium VI
239 was obtained. These results suggest an oxido-reduction process on the surface of the
240 nanoparticle. At these reaction conditions, the reduced Chromium is not liberated to the

241 medium; remains on the NPs surface. The presence of Ce^{3+} at the oxygen vacancy has
242 been reported [33].

243 To compare the adsorption capacity of the CeO_2 nanoparticles synthesized with
244 others adsorbents reported in the literature, the reaction conditions must be similar. In
245 Table 2 some previous values reported in the literature are compared. However, it
246 should be noted that it is not easy comparing adsorption results because the
247 experimental conditions are not the same. The NPs synthesized are not supported under
248 other material, all the surface area are available to adsorption process. Differences in the
249 synthesis process of NPs could change the physico-chemical properties of the surface.

250 CeO_2 nanoparticles synthesized adsorb 1.88 mg/g at low initial Cr(VI) concentration
251 adsorbate (0.6 g/ml and 320 mg/l Cr(VI) and CeO_2 respectively). This value is higher
252 than the adsorption capacity reported in the literature by Xiao et al. [19] (1.5 mg/l) even
253 though the initial concentration and adsorbate mass were almost two times smaller. At
254 the same equilibrium Cr(VI) concentration (15 mg/l Cr(VI)), Di et al. [18] showed that
255 the adsorption capacity of CeO_2 nanoparticles synthesized were higher than the values
256 reported. Yuan et al. [34] reported the use of Montmorillonite-supported magnetite
257 nanoparticles for Chromium removal even though the removal efficiency at pH closer to
258 7 is low. These results suggest the possibility of CeO_2 nanoparticles to be used for water
259 treatment process at pH 7 in a wide range of chromium concentration for drinking water
260 purification (small concentration levels of chromium (VI)) to industrial wastewater
261 treatment process to remove high concentration of chromium. Finally, it must be
262 pointed that HMT, as stabilizer, is added in excess in the reaction bath, while the
263 precursor of cerium atoms, cerium nitrate, is the limiting factor. However, according to
264 literature, HMT easily decomposes to formaldehyde and finally to ammonia ($NH_4^+OH^-$),
265 CO_2 and H_2O [35, 36].

266 The experimental data fit well the Freundlich adsorption isotherm model [29],
267 which represents the relationship between the amount of adsorbate 15.77 adsorbed per
268 unit mass of adsorbent (q_e) and the concentration of adsorbate at equilibrium (C_e), being
269 K and n are constants representing the adsorption capacity and intensity of the
270 adsorption (Equation 1):

$$271 \quad q_e = kC_e^{1/n} \quad (1)$$

272 The correlation coefficient obtained was $R^2 = 0.9554$ and n value was 2.1 and k
273 value was 20.57.

274

275 3.2. Pseudo-second-order kinetic model

276 A pseudo-second order model based on the assumption that the rate limiting step are the
277 chemical sorption involving valence forces through sharing or the exchange of electrons
278 between sorbent and sorbate [37] was used as kinetic model. The kinetics of the
279 sorption reaction has been described as a function of the sorption equilibrium capacity
280 (q_e), the initial metal ion concentration, the adsorbent dose and the nature of solute ion.

281 The pseudo-second-order rate constants (k_2) and the amount of Cr(VI) adsorbed
282 at equilibrium (q_e) were calculated experimentally by plotting (t/q_t) versus t according
283 to Equation 2. q_e is the amount of Cr(VI) adsorbed (mg/g) at equilibrium, and q_t is the
284 amount of the adsorption (mg/g) at any time t . The kinetics of the removal process is
285 shown in Figure 3.

$$286 \quad t/q_t = 1/k_2q_e^2 + (1/q_e)t \quad (2)$$

287 The obtained values fitted well according to this model (Table 3).

288

289 3.3. Cr(VI) desorption studies

290 The chromium desorption study was performed at neutral, acid and basic conditions
291 (deionized H₂O, 0.1M HNO₃, 0.1M HCl, 0.1M H₂SO₄ and 0.1M NaOH). The
292 chromium desorption at acid eluents have higher recovery percentage, around 100%
293 with H₂SO₄, 80% recovery with HCl and 86% with HNO₃ (Figure 4); however a
294 considerable redissolution of CeO₂ was detected (Figure 4).

295 The amount of Cr(VI) obtained using water as eluent could be the chromium physically
296 sorbed at the surface when the cerium-chromium particles were dried, before the
297 addition of the eluents. Regarding the cerium detected in deionized water eluent (5% of
298 the initial cerium) it could be due to nanoparticles suspended at the liquid phase. It is
299 evident that Cr VI ionic forms change with pH. However, one of the main advantages of
300 CeO₂ nanoparticles for adsorption process is the wide maximum adsorption as a
301 function of pH (from 3.0 to 7.4) [18]. A slight diminution of pH during the adsorption
302 process was observed, the final pH value after 24 hours was 6.5.

303 The chromium desorption process performed with NaOH as eluent was less efficient
304 (64% recovery) than the acid eluents but the amount of Ce in dissolution was minimum
305 0.07%. Probably at higher NaOH concentrations higher chromium desorption should be
306 produced; then the CeO₂ nanoparticles could be re-used without a complicated
307 separation process. In fact, After 24 hours desorption process treatment with 0.1M
308 NaOH solution, the NPs were separated by centrifugation process and were re-used for
309 Chromium removal (triplicate). 75% of Chromium removal was obtained in this second
310 cycle.

311 According to the obtained results desorption and regeneration of CeO₂
312 nanoparticles should only be feasible, from a practical point of view, in the case of basic
313 desorption.

314

315 *3.4 Transmission electron microscopy*

316 Transmission electron microscopy (TEM) images of initial CeO₂ nanoparticles are
317 shown in Figures 5a and 5b. Octahedral CeO₂ nanocrystals with a uniform size
318 distribution of 12 nm (Table 1) were obtained. A control sample was also performed
319 without the addition of Cr(VI) solution, with deionization water being used instead,
320 maintaining the same conditions of agitation and time than in the adsorption
321 experiments. These CeO₂ nanoparticles (Figure 5c) show a fine homogeneous
322 agglomerate of particles around 12 nm of diameter conformed by smaller rounded
323 nanoparticles with homogeneous size and morphology. A change in morphology was
324 observed without the addition of chromium VI solution. The octahedral nanocrystals of
325 the nanoparticles synthesized were not observed in the images of CeO₂ nanoparticles
326 with deionized water added. A diminution of nanoparticles size was also observed.
327 These morphology variations in the nanostructures are attributed to an intra-
328 agglomerate re-orientation to attain the low energy configuration [38]. TEM images of
329 CeO₂ nanoparticles after chromium (VI) adsorption showed the presence of spherical
330 homogeneous interconnected agglomerates with approximately 70 nm in diameter
331 (Figure 5d). These agglomerates are ensembles of spherical nanoparticles. An
332 estimation of the particle size is possible from a few isolated nanoparticles in the
333 periphery of the agglomerates (Figure 5e); the diameter particle is in the order of 2 nm.
334 However, an accurate measure of the particle size distribution of these nanoparticles
335 could not be obtained.

336 Figure 5f shows the homogeneous agglomeration of CeO₂ nanoparticles
337 obtained after desorption treatment using 0.1M NaOH as eluent. 80 nm agglomerated
338 diameter and 4 nm nanoparticles approximately in diameter were measured.
339 Electrostatic forces between these particles could result in particle agglomeration.

340

341 *3.5 Adsorption mechanism*

342 The CeO₂ nanoparticles with a positive charge (Z potential 11.5 mV) were
343 stabilized via electrostatic repulsion with a covered hexamethylenetetramine molecules
344 shell on the particle surface. When the chromium (VI) solution was added to the
345 nanoparticles, a brownish agglomerate was immediately observed. Attractive forces
346 (e.g. induced dipole interaction, Van der Waals force, hydrogen bonds, bi- or
347 multivalent, oppositely charged ions or polyelectrolytes) can bridge the particles by
348 electrostatic attraction, causing destabilization of the nanoparticles [39, 40]. In this case
349 the presence of chromium ions in solution could destabilize the nanoparticles
350 dispersion, reacting and forming aggregates. The charge and the species in solution is
351 one of the most important issues in agglomeration phenomena, in the case of chromium
352 (VI) solutions, the solution species are a function of the pH and total Cr concentration
353 [41]. At pH 7 the major species in solution are HCrO₄⁻ and CrO₄²⁻. The charge attraction
354 of the chromium anions to the positive charged nanoparticles could be the first step
355 process, then a chemisorption process could proceed and a multibranch homogeneous
356 in size and shape network is formed with the chromium ions acting as a bridge between
357 different CeO₂ nanoparticles surface via an anionic interchange between the ionic
358 chromium species and the hydroxylation surface [10]. Nevertheless, the heterogeneous
359 metal oxide surface, for example oxygen vacancy, step edges [42, 43] and small
360 amounts of Ce³⁺ on the surface remaining from the reaction synthesis could contribute
361 to the Chromium elimination by chromium reduction process.
362 The stability of the aggregates formed still remains after basic desorption treatment. In
363 any case, the agglomeration of the CeO₂ nanoparticles provides an easy way to remove

364 the product in order to separate and re-use the CeO₂ nanoparticles and to obtain a
365 concentrated chromium solution by desorption.

366

367 3.6. Bioluminescent test

368 The bioluminescent test is broadly used to evaluate the potential harmful effects of
369 effluents discharged into surface waters [25]. Some proposed regulations set limit
370 values for bioluminescent toxicity at 25 Equitox/m³ [45]. The IC₅₀ obtained for the
371 Cr(VI) solution was 1.92 mg/l at 5 min exposure time (Table 4). In the case of CeO₂
372 nanoparticles the IC₅₀ value obtained was 21.76 mg/l. The CeO₂ nanoparticles are
373 positively charged at neutral pH and thus display a strong electrostatic attraction
374 towards bacterial outer membranes. In this sense, Thill et al. [46] suggest that the first
375 step for toxicity in *E. Coli* bacteria is the adsorption of it by the CeO₂ nanoparticles. The
376 authors's study concluded that direct contact between the *E. coli* and the CeO₂
377 nanoparticles need to be assumed for CeO₂ cytotoxicity to occur and that the reduction
378 of the nanoparticles occurs at or close to the surface of the bacteria and may be
379 associated with cytotoxicity. The toxicity of the suspension obtained from an
380 adsorption process after 3 hours of reaction (37.5 mg/l of initial chromium) was 19.72
381 mg/l at 5 min exposure time. The differences between them (21.76 mg/l and 19.72 mg/l)
382 and the high toxicity of the chromium solution (1.92 mg/l) suggest that the chromium
383 adsorbed on the CeO₂ nanoparticles reduce the intrinsic chromium toxicity against the
384 bacteria tested. Even though after 15 minutes of exposure time the IC₅₀ diminish to
385 13.6 mg/l, and the IC₅₀ for chromium solution also diminish at this time. A study of the
386 toxicity of these nanoparticles at longer periods of time has to be done in order to know
387 the possible environment impact. A dissolution process or aggregation phenomenon has
388 to be in account.

389

390 **4. Conclusions**

391 The results obtained in this study demonstrate that the use of the cerium oxide
392 nanoparticles synthesized can be an excellent option for the removal of low amounts of
393 dissolved chromium VI in the purification of drinking water or in the re-use of
394 wastewater. The agglomeration of nanoparticles during the adsorption process allows
395 the use of common technologies in wastewater procedure to eliminate them. The
396 adsorption of chromium onto nanoparticles is well described by the Freundlich
397 isotherm, whereas kinetics corresponds to a pseudo-second order equation. Both facts
398 ensure a practically complete removal of chromium under the conditions tested.
399 Following the treatment process, nanoparticles can be removed from water by
400 centrifugation, whereas chromium can be desorbed using sodium hydroxide, closing
401 the cycle of chromium removal, although some morphological changes are observed in
402 the nanoparticles used. Of course, other parameters influencing the adsorption process
403 such as pH, ionic strength, and temperature can be the object of further studies. Finally, the
404 toxicity of the resulting solutions is not significantly altered using this treatment.

405

406 **Acknowledgements**

407 Financial support was provided by the Spanish Ministerio de Medio Ambiente y Medio
408 Rural y Marino (Project Exp. 007/RN08/03.1). Sonia Recillas and Joan Colón thank
409 Universitat Autònoma de Barcelona for the award of a post-doctoral and pre-doctoral
410 fellowship respectively.

411

412 **References**

- 413 [1] N. Ichinose, Y. Ozaki, S. Kashu, Superfine particle technology, Springer,
414 London, 1992.
- 415 [2] P.V. Kamat, Photophysical, photochemical and photocatalytic aspects of metal
416 nanoparticule, J. Phys. Chem. B. 106 (2002)7729-7744.
- 417 [3] P.K. Stoimenov, R.L. Klinger, G.L. Marchin, K.J. Klabunde, Metal oxide
418 nanoparticles as bactericidal agents, Langmuir 18 (2002) 6679-6686.
- 419 [4] S.W. Cao, Y.J. Zhu, Hierarchically nanostructured α -Fe₂O₃ hollow spheres:
420 preparation, growth mechanism, photocatalytic property, and application in
421 water treatment. J. Phys. Chem. C. 112 (2008) 6253-6257.
- 422 [5] H.M. Chen, J.H. He, Facile synthesis of monodisperse Manganese Oxide
423 nanostructures and their application in water treatment. J. Phys. Chem. C. 112
424 (2008) 17540-17545.
- 425 [6] D.K Tiwari, J. Behari, P. Sen, Application of nanoparticles in waste water
426 treatment. World Appl. Sci. J. 3 (2008) 417-433.
- 427 [7] D. Paustenbach, B. Finley, F. Mowat, B. Kerger, Human Health Risk and
428 Exposure Assessment of Chromium (VI) in Tap Water, J. Toxicol. Environ.
429 Health Part A, 66 (2003) 1295-1339.
- 430 [8] Council Directive 98/83/EC of 3 November 1998, on the quality of water
431 intended for human consumption. Official Journal L 330 , 05/12/1998 P. 0032 –
432 0054.
- 433 [9] M.A. Olazabal, N.P. Nikolaidis, S.A. Suib, J.M. Madariaga, Precipitation
434 equilibria of the Chromium(VI)/Iron(III) system and spectroscopic
435 characterization of the precipitates. Environ. Sci. Technol. 31 (1997) 2898-2902
- 436 [10] Z.H. Ai, Y. Chen, L.Z. Zhang, J.R. Qiu, Efficient removal of Cr(VI) from
437 aqueous solution with Fe@Fe₂O₃ Core-Shell Nanowires. Environ. Sci. Technol.
438 42 (2008) 6955-6960.
- 439 [11] M.J.S. Yabe, E. Oliveira, Heavy metals removal in industrial effluents by
440 sequential adsorbent treatment. Adv. Environ. Res. 7, (2003) 263-272.
- 441 [12] P.A. Kumar, M. Ray, S. Chakraborty, Hexavalent chromium removal from
442 wastewater using aniline formaldehyde condensate coated silica gel. J. Hazard.
443 Mater. 143 (2007) 24-32.

- 444 [13] K. Selvi, S. Pattabhi, K. Kadirvelu, Removal of Cr(VI) from aqueous solution
445 by adsorption onto activated carbon. *Bioresour. Technol.* 80 (2001) 87-89.
- 446 [14] Z. Hu, L. Lei, Y. Li, Y. Ni, Chromium adsorption of high performance activated
447 carbon from aqueous solution. *Sep. Purif. Technol.* 31 (2003) 13-18.
- 448 [15] S.E. Bailey, T.J. Olin, R.M. Bricka, D.D. Adrian, A review of potentially low-
449 cost sorbents for heavy metals. *Water Res.* 33 (1999) 2469-2479.
- 450 [16] S-H. Huang, D-H. Chen, Rapid removal of heavy metal cations and anions from
451 aqueous solutions by an amino-functionalized magnetic nano-adsorbent, *J.*
452 *Hazard. Mater.* 163 (2009) 174-179.
- 453 [17] L-S. Zhong, J-S. Hu, A-M. Cao, Q. Liu, W-G. Song, L-J. Wan, 3D Flowerlike
454 Ceria Micro/Nanocomposite Structure and Its Application for Water Treatment
455 and CO Removal, *Chem. Mater.* 19 (2007) 1648-1655.
- 456 [18] Z.C. Di, J. Ding, X.J. Peng, Y.H. Li, Z.K. Luan, J. Liang, Chromium adsorption
457 by aligned carbon nanotubes supported ceria nanoparticles, *Chemosphere* 62
458 (2006) 861-865.
- 459 [19] H.I. Xiao, Z.H. Ai, L.Z. Zhang, Nonaqueous Sol-Gel synthesized hierarchical
460 CeO₂ nanocrystal microspheres as novel adsorbents for wastewater treatment, *J.*
461 *Phys. Chem. C.* 113(38) (2009) 16625-16630.
- 462 [20] S.C. Laha, R. Ryoo, Synthesis of thermally stable mesoporous cerium oxide
463 with nanocrystalline frameworks using mesoporous silica templates, *Chem.*
464 *Commun.* 17 (2003) 2138-2139.
- 465 [21] S.C. Kuiry, S. Patil, S. Deshpande, S. Seal, Spontaneous self-assembly of
466 cerium oxide nanoparticles to nanorods through supraaggregate formation, *J.*
467 *Phys. Chem. B.* 109 (2005) 6936-6939.
- 468 [22] M. Gutierrez, J. Etxebarria, L. Fuentes, Evaluation of wastewater toxicity:
469 comparative study between Microtox® and activated sludge oxygen uptake
470 inhibition, *Water Res.* 36 (2002) 919-924.
- 471 [23] F. Zhang, Q. Jin, S.W. Chan, Ceria nanoparticles: Size, size distribution, and
472 shape, *J. Appl. Phys.* 95 (2004) 4319-4326
- 473 [24] A. Greenberg, J. Connors, D. Jenkins, Standard methods for the examination of
474 water and wastewater. 15th ed. American Public Health Association, USA. 187-
475 190, 1981.

- 476 [25] DIN 38412, part 34, 1991. Determination of the inhibitory effect of wastewater
477 on the light emission of *Photobacterium phosphoreum* (test using preserved
478 luminescent bacteria).
- 479 [26] A.K. Pandey, V. Misra, A.K. Srimal, Removal of chromium and reduction of
480 toxicity to Microtox system from tannery effluent by the use of calcium alginate
481 beads containing humic acid, *Chemosphere* 51 (2003) 329–333.
- 482 [27] A. Trovarelli, *Catalysis by Ceria and related materials*. Imperial College Press,
483 London, 2002.
- 484 [28] C.R. Stanek, A.H.H. Tan, S.L. Owens, R.W. Grimes, Atomistic simulation of
485 CeO₂ surface hydroxylation: implications for glass polishing. *J Mater Sci.* 43
486 (2008) 4157-4162.
- 487 [29] S. Bernal, J.J. Calvino, M.A. Cauqui, J.M. Gatica, C. Larese, J.A. Pérez Omil,
488 J.M. Pintado, Some recent results on metal/support interaction effects in
489 NM/CeO₂ (NM: noble metal) catalysts, *Catal. Today* 50 (1999) 175-206.
- 490 [30] S. Carretin, P. Concepción, A. Corma, J.M. López Nieto, V.F. Puentes,
491 Nanocrystalline CeO₂ Increases the Activity of Au for CO Oxidation by Two
492 Orders of Magnitude. *Angew. Chem. Int. Ed.* 43 (2004) 2538-2540.
- 493 [31] F. Esch, S. Fabris, L. Zhou, T. Montini, C. Africh, P. Fornasiero, G. Comelli, R.
494 Rosei, Electron localization determines defect formation on ceria substrates.
495 *Science* 309 (2005) 752-755.
- 496 [32] J.Y. Chane-Ching, M. Airiau, A. Sahibed-dine, M. Daturi, E. Brendlé, F. Ozil,
497 A. Thorel, A. Corma, Surface Characterization and Properties of Ordered Arrays
498 of CeO₂ Nanoparticles Embedded in Thin Layers of SiO₂. *Langmuir* 21 (2005)
499 1568-1574.
- 500 [33] E.G. Heckert, S. Seal, W.T. Self, Fenton-like reaction catalyzed by the rare earth
501 inner transition metal cerium, *Environ. Sci. Technol.* 42 (2008) 5014-5019.
- 502 [34] P. Yuan, M. Fan, D. Yang, H. He, D. Liu, A. Yuan, J. Zhu, T. Chen,
503 Montmorillonite-supported magnetite nanoparticles for the removal of
504 hexavalent chromium [Cr(VI)] from aqueous Solutions. *J. Hazar. Mat.* 166
505 (2009) 821-829.
- 506 [35] J.G. Strom Jr., H.Won Jun, Kinetics of hydrolysis of methenamine. *J. Pharm.*
507 *Sci.* 69 (1980) 1261-1263.

508 [36] A.J. Allen, V.A. Hackley, P.R. Jemian, J. Ilavsky, J.M. Raitano, S.-W. Chan, In
509 situ ultra-small-angle X-ray scattering study of the solution-mediated formation
510 and growth of nanocrystalline ceria. *J. Appl. Cryst.* 41 (2008) 918-929.

511 [37] I. Langmuir, The adsorption of gases on plane surfaces of glass, mica and
512 platinum. *J. Am. Chem. Soc.* 40 (1918) 1361-1403.

513 [38] Y.S. Ho, G. McKay, The kinetics of sorption of divalent metal ions onto
514 sphagnum moss peat, *Water Res.* 34 (2000) 735-742.

515 [39] S.V.N.T. Kuchibhatla, A.S. Karakoti, S. Seal, Hierarchical assembly of
516 inorganic nanostructure building blocks to octahedral superstructures-a true
517 template-free self-assembly, *Nanotechnology* 18 (2007) 075303.

518 [40] K. Kimura, S. Takashima, H. Ohshima, Molecular approach to the surface
519 potential estimate of thiolate-modified gold nanoparticles, *J. Phys. Chem. B.*
520 106 (2002) 7260-7266.

521 [41] T. Laaksonen, P. Ahonen, C. Johans, K. Kontturi, Stability and electrostatics of
522 mercaptoundecanoic acid-capped gold nanoparticles with varying counterion
523 size. *Chemphyschem* 7 (2006) 2143-2149.

524 [42] B. Mukhopadhyaya, J. Sundq, R.J. Schmitzc, Removal of Cr(VI) from Cr-
525 contaminated groundwater through electrochemical addition of Fe(II), *J.*
526 *Environ. Manag.* 82 (2007) 66-76.

527 [43] C.T. Campbell, and C.H.F. Peden, Oxygen vacancies and catalysis on ceria
528 surfaces, *Science* 309 (2005) 752-755.

529 [44] F. Esch, S. Fabris, L. Zhou, T. Montini, C. Africh, P. Fornasiero, G. Comelli, R.
530 Rosei, Electron localization determines defect formation on Ceria substrates,
531 *Science* 309 (2005) 752-755.

532 [45] R. Barrena, E. Casals, J. Colón, X. Font, A. Sánchez, V. Puentes, Evaluation of
533 model nanoparticles eco-toxicity, *Chemosphere* 75 (2009) 850-857.

534 [46] A. Thill, O. Zeyons, O. Spalla, F. Chauvat, J. Rose, M. Auffan, A.M. Flank,
535 Cytotoxicity of CeO₂ nanoparticles for *Escherichia col.*, *Environ. Sci. Technol.*
536 40 (2006) 6151-6156.

537

538

539

540

541 **Tables**

542

543 **Table 1.-** Main characteristics of the used CeO₂ nanoparticles.

544

CeO₂ nanoparticle	
Concentration (mg/ml)	0.64
Mean size (nm)	12
Shape	shapeless
Zeta potential (mV)	+11.5
Stabilizer*	HMT
Stabilizer concentration (mM)	8.3
pH (original)	9
Surface BET area (m ² /g)	65

545

546

*HMT: Hexa Methyl Tetramine

547

548

549

550

551

552

553

554

555

556

557

558

559 **Table 2.-** Maximum Chromium (VI) sorption capacity of various adsorbents.

560

Adsorbent	Adsorbent capacity (mg Cr(VI)/g adsorbent)	Initial Cr(VI) concentration (mg/l)	Equilibrium Cr(VI) concentration (mg/l)	Initial adsorbent concentration (g/l)	References
Synthesized CeO ₂ nanoparticles	1.88	0.6		0.320	This work
Synthesized CeO ₂ nanoparticles	83.33	37.5		0.320	This work
Synthesized CeO ₂ nanoparticles	121.95	80		0.320	This work
Cerium microsphere	1.5	2		1	[18]
Commercial Cerium	0.37				[18]
Synthesized CeO ₂ nanoparticles	70.41		15		[17]
CeO ₂ /ACNTs	26		15		[17]
Activated carbon EA-200	10		15		[17]
γ Al ₂ O ₃	7.5		15		[17]

561

562

563

564 **Table 3.-** Maximum adsorption capacity at equilibrium and pseudo-second-order rate

565 constants (k_2) obtained using the pseudo-second-order kinetic model for 0.6, 37.5 and

566 80 mg/l initial Cr(VI) concentration.

567

Cr(VI) initial (mg/l)	q_e (mgCr(VI)/gCeO ₂)	k_2 (g CeO ₂ /mgCr(VI).min)	R^2
0.6	1.88	0.2525	1
37.5	83.33	0.012	0.9998
80	121.95	0.0082	0.9992

568

569

570

571

572

573

574

575

576

577

578

579

580

581

582

Pre-print

583

584 **Table 4.-** Half maximal inhibitory concentration (IC₅₀) of a 30 mg/l Chromium
585 solution, initial CeO₂ nanoparticles and CeO₂-Cr(VI) suspension.

586

Compounds	IC ₅₀ (mg/l)	
	5 min	15 min
Cr(VI) solution	1.92	1.2
CeO ₂ nanoparticles suspension	21.76	25.16
CeO ₂ -Cr(VI) suspension	19.72	13.6

587

588

589

590

591

592

593

594

595

596

Pre-print

597 **Legends to Figures**

598

599 **Figure 1.-** X-Ray Diffraction spectra (a) and size distribution (b) of CeO₂ nanoparticles.

600 **Figure 2.-** Chromium adsorption evolution at pH=7 and room temperature. Initial
601 Cr(VI) concentrations are 0.6 (circle), 37.5 (square), 80 mg/l (triangle).

602 **Figure 3.-** Adsorption pseudo-second-order kinetic model for Chromium adsorption at
603 pH=7 and room temperature. Initial Cr(VI) concentrations are 0.6 (circle), 37.5
604 (square), 80 mg/l (triangle).

605 **Figure 4.-** Chromium (VI) desorption from nanoparticles of CeO₂ after 3 hours of
606 reaction with different eluents (black bars) and percentage of the initial cerium
607 dissolved after desorption experiments, analyzed by ICP-MAS (white bars).

608 **Figure 5.-** TEM images of the initial CeO₂ nanoparticles (a and b); control CeO₂
609 nanoparticles in deionized water (c); CeO₂ nanoparticles after adsorption of Chromium
610 (VI) at different amplifications (d and e) and CeO₂ nanoparticles after desorption with
611 0.1M NaOH eluent (e).

612

613

614

615

616

617 Figure 1

618

619

620

621

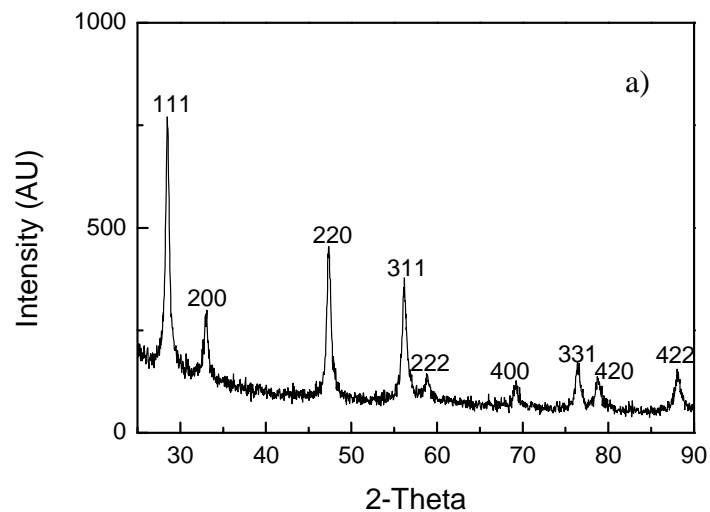
622

623

624

625

626

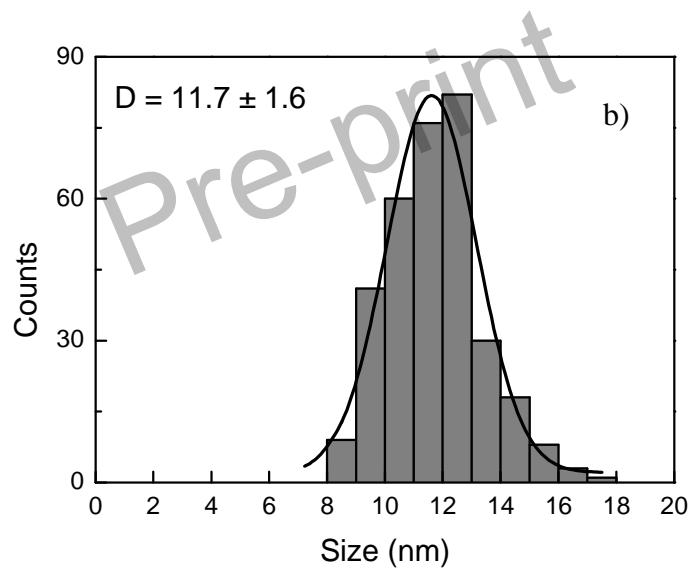


627

628

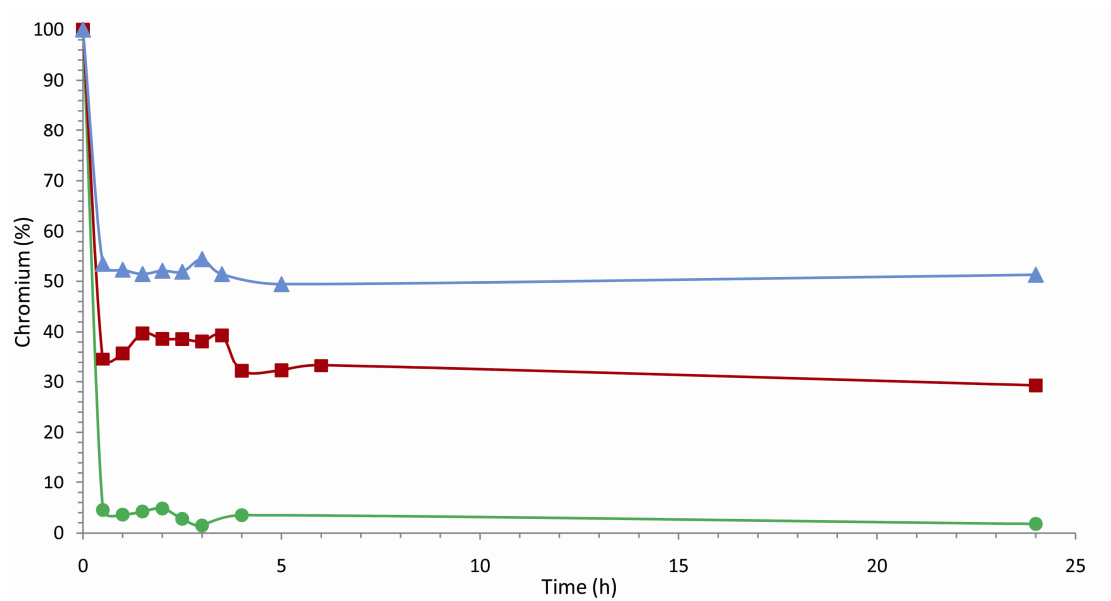
629

630



631 Figure 2

632



633

634

635

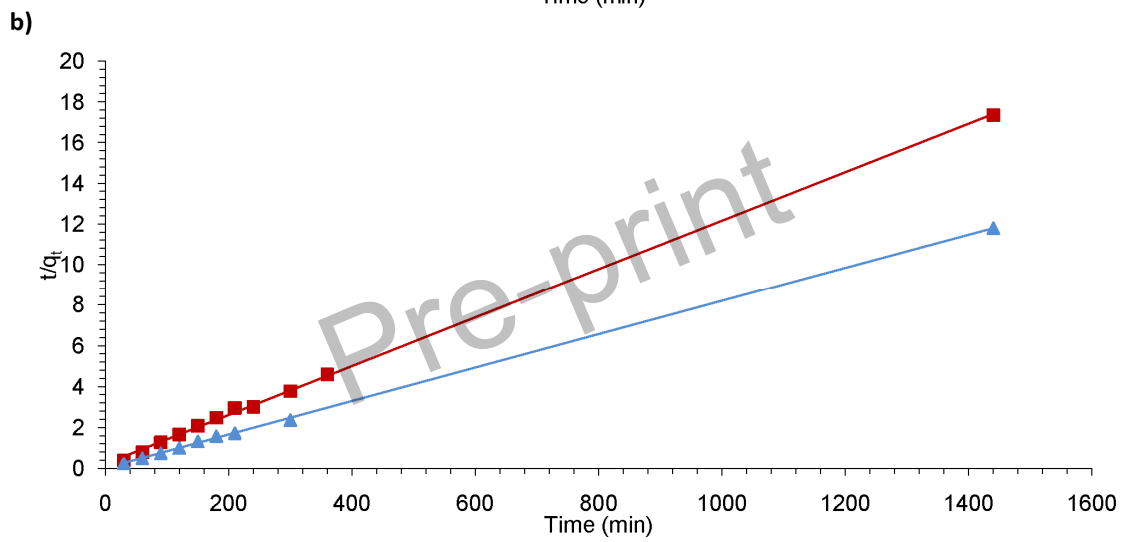
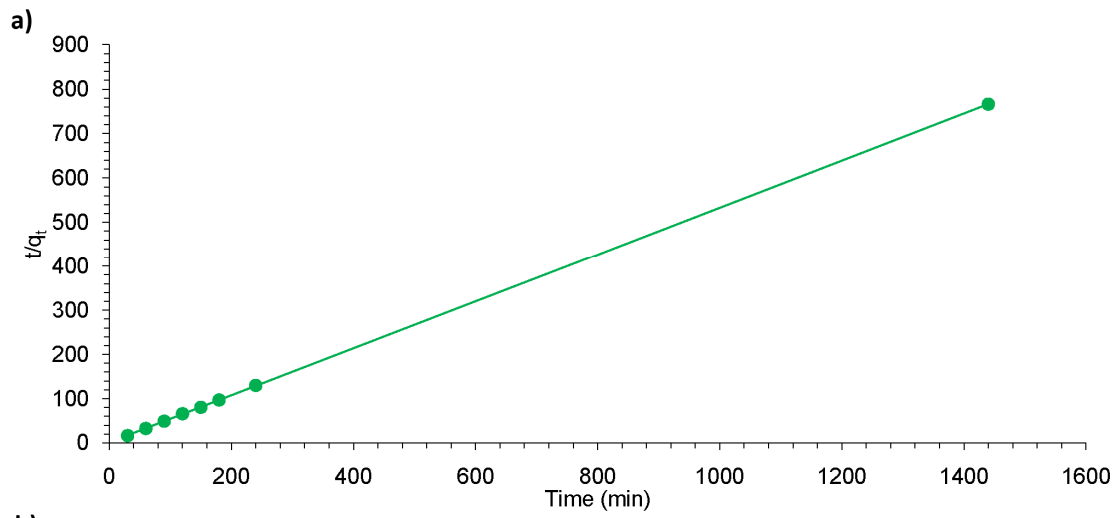
636

637

Pre-print

638 Figure 3

639



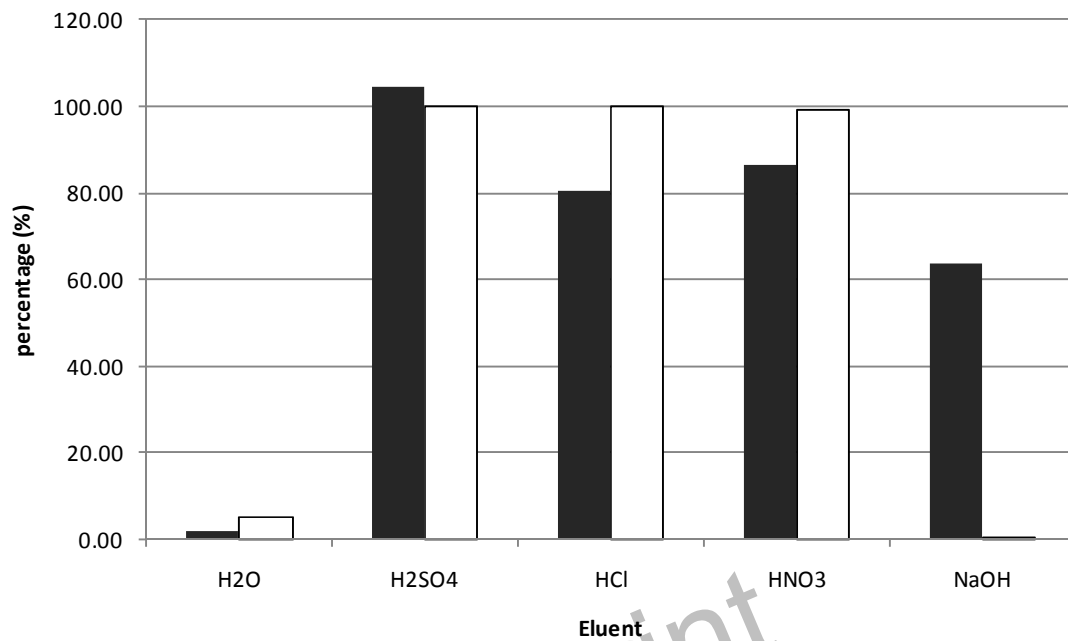
640

641

642 Figure 4

643

644



645

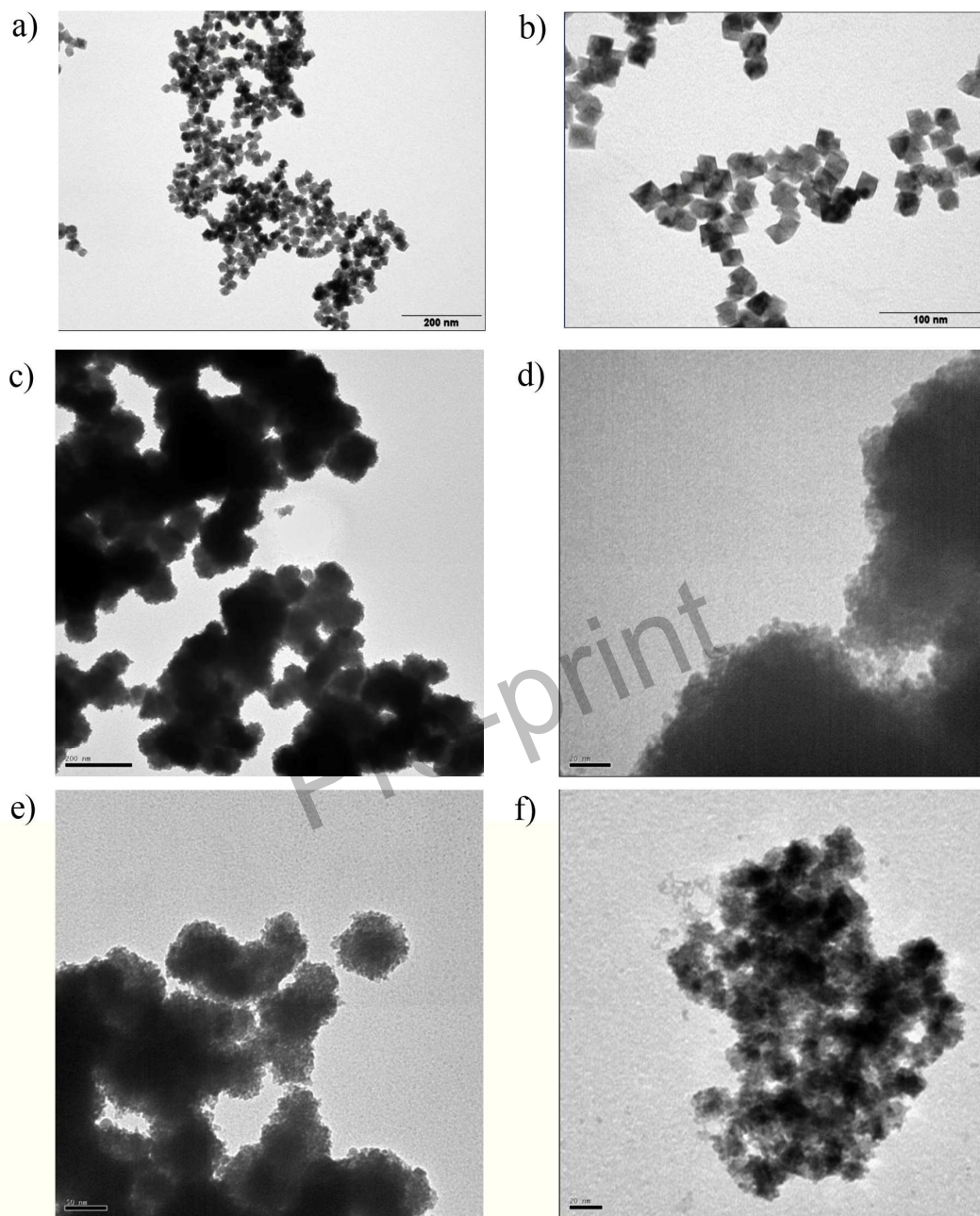
646

647

Pre-print

648 Figure 5

649



650

651